

REVISTA TECNICA

DE LA FACULTAD DE INGENIERIA
UNIVERSIDAD DEL ZULIA

MARACAIBO - VENEZUELA



Una Revista Internacional Arbitrada
que está indizada en las publicaciones
de referencia y comentarios:

- Science Citation Index (SCIExpanded)
- Compendex
- Chemical Abstracts
- Metal Abstracts
- World Aluminium Abstracts
- Mathematical Reviews
- Petroleum Abstracts
- Current Mathematical Publications
- MathSci (online database)
- Revenct
- Materials Information
- Periódica
- Actualidad Iberoamericana

Axial Stress Prediction of Torsioned Solid and Hollow Cylindrical Bars

Gustavo González, Verónica Di Graci, Omar Zurita, María Capace

*Department of Mechanics, Simon Bolivar University, Caracas, Venezuela

Abstract

A simple methodology is proposed for the prediction of axial tensile yield and ultimate strength of solid and hollow cylindrical bars previously cold worked by means of a torsion process, based on the assumption of an angle of twist. For the validation of the method annealed AISI 1020 and AISI 1045 steel samples were torsioned under different angles of twist. The AISI 1020 samples were later drilled to remove the core, and all were subjected to tensile tests to measure the yield and ultimate strength. As expected, it was found that the strength increased with the angle of twist, and that hollow samples have even higher strength values than the solid ones. The proposed formulation showed good accuracy with errors not greater than 9.78 and 6.81% for solid and hollow samples, respectively.

Keywords: cylindrical bars; torsion; angle of twist; ultimate strength; yield strength.

Predicción de Resistencia Axial en Barras Cilíndricas Sólidas y Huecas Torsionadas

Resumen

Se propone una metodología simple para la predicción de la resistencia a fluencia y máxima a la tracción axial de barras cilíndricas sólidas y huecas previamente trabajadas en frío por medio de un proceso de torsión, basada en la suposición de un ángulo de torsión. Para la validación del método muestras de acero recocido AISI 1020 y AISI 1045 se torsionaron bajo diferentes ángulos de torsión. Las muestras de AISI 1020 fueron posteriormente perforadas para eliminar el núcleo, y todas fueron sometidas a ensayos de tracción para medir resistencia a fluencia y máxima. Como se esperaba, se encontró que la resistencia aumentaba con el ángulo de torsión, y que las muestras huecas tenían valores de resistencia incluso mayores que los sólidos. La formulación propuesta mostró una buena precisión con errores no superiores a 9,78 y 6,81% para muestras sólidas y huecas, respectivamente.

Palabras clave: barras cilíndricas; torsión; ángulo de torsión; resistencia máxima; resistencia a fluencia.

Introduction

In metal forming processes, torsion of solid or hollow specimens is used to obtain high plastic strain rates, without significant dimensional changes in diameter and length. By twisting, the internal structure of mechanical components can be conveniently altered, and is recommended as it raises the yield and tensile strength of the parts such as shafts, axles, and twist drills. Consequently, as reported by Knap [1], knowledge of the residual stresses resulting from the working processes is particularly important.

Numerous studies have been conducted to determine relationships between the torsion process and mechanical properties. Yang and Welzel [2], using X-ray diffraction line broadening, transmission electron microscopy and microhardness techniques on Ni samples, quantified the distribution of grain size and microstrain along the radial direction of torsioned disks. They observed that a gradient in microhardness exists, showing the higher values in the outer region, as a result of a slightly smaller grain size, and a more homogeneous microstructure at the periphery.

Experiments conducted to evaluate the effect of torsion on an aluminum alloy and pure copper, by Horita and Langdon

[3], showed that significant grain refinement is achieved in both materials with grain sizes of 150 and 140 μm , respectively. They also reported that microhardness measurements demonstrated increases in the values near the edges of the disks by factors of approximately three and two for these materials, respectively.

Recently, Janecek et al. [4] applied torsion to samples of ultrafine-grained interstitial free steel. They found that, after 0.5 turns, the disc center has the lowest hardness value, and the hardness increases almost linearly from the center to the edge, reaching a maximum value at the edge. Most of these results were confirmed by Huang et al. [5] by torsion in pure tantalum. A study by Jiang et al. [6] on torsion of a Ti5553 alloy showed that the hardness and ultimate tensile strength increased by processing, accompanied by a decrease in the elongation to failure.

Empirically based approaches have been carried out to interpret torsional data, and convert them into intrinsic stress/strain relationships, but this process is not always straightforward.

Canova et al. [7] proposed a method to perform the derivation of the shear stress/shear strain curve from the torque/twist data, and convert the former curve into an equivalent stress/equivalent strain relationship. They showed that, when the corrected conversions were used, the rate of work hardening calculated from torsion tests was lower than the achieved from uniaxial testing.

Employing a torsion test on a solid cylinder, Batdorf and Ko Robert [8], showed that the exact solution for finding the shear stress/strain relation of a material is easily obtained as a correction to the quasielastic approximation. The proposed solution is extended to the case of hollow cylinders and is also applicable to conditions where a constant axial stress is presented.

A simple formulation is presented by Hematiyan and Doostfatemeh [9] for torsion analysis of hollow tubes with polygonal shapes, in which the thicknesses of segments of the cross section can be different. To derive the formulas, governing equations in term of Prandtl's stress function where used. They presented several examples to show the accuracy and efficiency of the formulation and the obtained results were also verified by accurate finite element solutions. The results demonstrated that the proposed formulas can be useful for analysis of thin-walled and moderately thick-walled hollow tubes.

Yang et al. [10] developed an analytical based recursive procedure solution for analysis of hollow cylindrical specimens under torsion, and an analytical solution was directly employed for solid torsional specimens. Examples related to these two cases were examined, and the resulting shear stress/strain curves compared with those based on a number of empirical methods. They conclude that the proposed analytical approaches can serve as a benchmark for checking the accuracy and validity of those empirical propositions.

From the literature stated above, it becomes clear that studies have been carried out by various researchers. Still there remains some importance to gain a better understanding of how the torsion manufacturing process affects the functional behavior of parts. Therefore, the aim of this study is to develop a simple formulation for the prediction of axial stress/strain relationship in torsion analysis. In the methodology, an angle of twist is assumed for shear stress through the solid or hollow cylindrical bars. The derived formulas are simple enough to be carried out with a calculator.

Experimental Procedure

Proposed Methodology

Upon submitting a cylindrical bar to a torsion process, due to the conservation of volume, the initial diameter and length do not change, and the longitudinal deformation of the fibers increases with the radius, thus the hardening in the surface of the bar is higher than in the interior, becoming almost zero at its center.

Assuming that at a radius (r) from the center of the bar is a horizontal fiber pa of length (l_a) (Figure 1). Arbitrarily selecting a point b , so that pb has a length (l_b), and lies at an angle (α) above pa . After rotating the right end of the cylinder an angle (θ), point b moves to c , so the fiber pb will be deformed to pc at an angle (γ), remaining with a final length (l).

The three-dimensional geometry of Figure 1 can be better appreciated as a planar surface in Figure 2, and from both the necessary relations can be obtained to calculate the longitudinal strain experienced by the fiber in study upon being displaced from pb to pc [11].

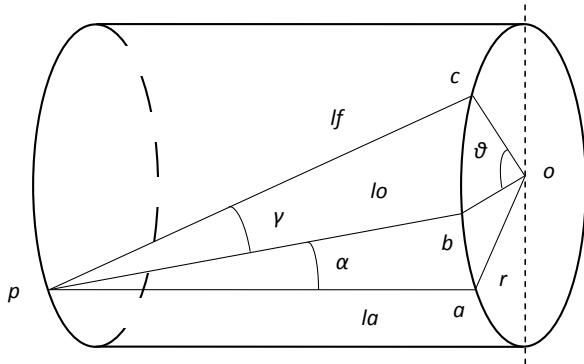


Figure 1. Torsion of a bar

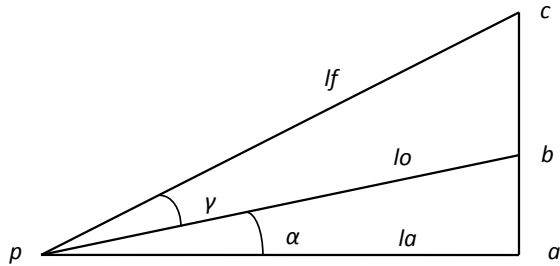


Figure 2. Geometric relations of a bar under torsion

The initial length of the fiber (l_o) is defined as:

$$l_o = \frac{l_a}{\cos(\alpha)} \tag{1}$$

After torsion, the final length (l_f) can be obtained as follows:

$$l_f = \sqrt{l_a^2 + (\overline{ab} + \overline{bc})^2} \tag{2}$$

$$\overline{ab} = l_a \cdot \text{tg}(\alpha) \tag{3}$$

$$\overline{bc} = r \cdot \theta \tag{4}$$

Substituting Eq. (3) and Eq. (4) in Eq. (2) results in:

$$l_f = \sqrt{l_a^2 + (l_a \cdot \text{tg}(\alpha) + r \cdot \theta)^2} \tag{5}$$

From the definition for strain, using Eq. (1) and Eq. (5), comes:

$$\varepsilon_{\text{tor}} = \ln \left(\frac{\sqrt{l_a^2 + (l_a \cdot \text{tg}(\alpha) + r \cdot \theta)^2}}{\frac{l_a}{\cos(\alpha)}} \right) \tag{6}$$

By differentiating Eq. 6 in relation to the angle (α), and equating the result to zero, it is possible to determine the value of angle (α) that gives the largest strain for any amount of angle of twist (θ). The obtained formula is expressed as follows:

$$\alpha = \frac{1}{2} \text{arctg} \left(\frac{2l_a}{r \cdot \theta} \right) \tag{7}$$

The fiber with higher strain is located at an angle (ϕ) with regard to the horizontal (Figure 3). The formula for angle (ϕ) is defined as:

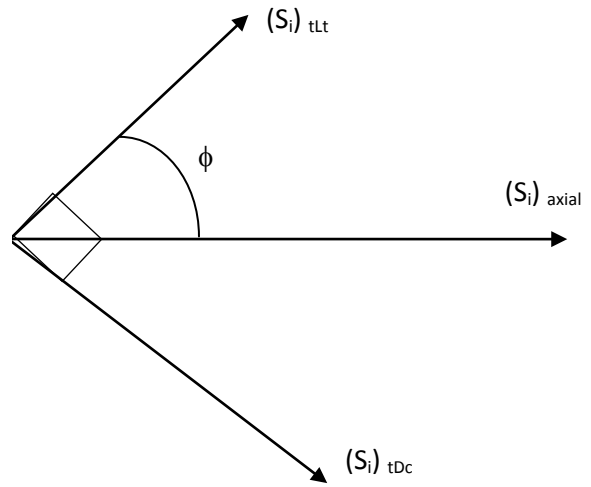


Figure 3. Stress distribution in the external surface of the bar

$$\phi = \text{arctg} \left(\frac{\overline{ab} + \overline{bc}}{l_a} \right) \tag{8}$$

Substituting Eq. (3) and Eq. (4) in Eq. (8) gives:

$$\phi = \arctg\left(\operatorname{tg}(\alpha) + \frac{r \cdot \theta}{l_a}\right) \quad (9)$$

The longitudinal strength of this fiber will be (Si)t ϕ t or (Si)tLt (tensile strength in ϕ), a fiber at 90° will be under compression, with a strength (Si)t(90- ϕ)c or (Si)tDc (Figure 3).

Then the axial strength (Si)axial can be expressed as:

$$(S_i)_{axial} = \frac{90-\phi}{90}(S_i)_{tLt} + \frac{\phi}{90}(S_i)_{tDc} \quad (10)$$

Axial Ultimate Strength

The longitudinal ultimate strength of the higher strained fiber (Su)tLt in term of Datsko's equivalent ulastic strain functions [11], for a bar annealed before torsion, can be written out as follows:

$$\begin{cases} \varepsilon_{qus} < m \Rightarrow (S_u)_{tLt} = S_{uo} \cdot e^{\varepsilon_{qus}} \\ \varepsilon_{qus} > m \Rightarrow (S_u)_{tLt} = \sigma_o (\varepsilon_{qus})^m \end{cases} \quad (11)$$

where the equivalent strain is:

$$\varepsilon_{qus} = \varepsilon_{tor} \quad (12)$$

For the compressed fiber at 90°, the ultimate strength (Su)tDc can be obtained as:

$$\begin{cases} \varepsilon_{quo} < m \Rightarrow (S_u)_{tDc} = S_{uo} \cdot e^{\varepsilon_{quo}} \\ \varepsilon_{quo} > m \Rightarrow (S_u)_{tDc} = \sigma_o (\varepsilon_{quo})^m \end{cases} \quad (13)$$

where:

$$\varepsilon_{quo} = \frac{\varepsilon_{tor}}{2} \quad (14)$$

Axial Yield Strength

The relation for longitudinal yield strength (Sy)tLt, again in term of Datsko's equivalent ulastic strain functions [11], of the higher strained fiber in a bar annealed before torsion, can be represented by the following equation:

$$(S_y)_{tLt} = \sigma_o (\varepsilon_{qys})^m \quad (15)$$

where the equivalent strain is:

$$\varepsilon_{qys} = \frac{\varepsilon_{qus}}{1 + 0,2 \cdot \varepsilon_{qus}} \quad (16)$$

The strength (Sy)tDc for the compressed fiber at 90°, can be expressed as:

$$(S_y)_{tDc} = \sigma_o (\varepsilon_{qyo})^m \quad (17)$$

where:

$$\varepsilon_{qyo} = \frac{\varepsilon_{quo}}{1 + 2 \cdot \varepsilon_{quo}} \quad (18)$$

Axial Mean Strength

In a twisted hollow cylindrical bar, for any angle (θ), two angles (α_1) and (α_2) will be present, given the radius (r_1) y (r_2), respectively. To evaluate the axial mean strength (S_p)^{axial (ri)}, two axial strength (S_p)^{axial (ri)} and (S_p)^{axial (re)} must be calculated, for the external (r_e) and internal (r_i) surfaces (Figure 4).

This can be achieved using the second theorem of Pappus, that states: "The volume V of a solid of revolution generated by the revolution of a lamina about an external axis is equal to the product of the area A of the lamina and the distance d traveled by the lamina's geometric centroid \bar{x} " [12].

The volume of the triangular torus generated by the revolution of (S_p)^{axial (ri)} and (S_p)^{axial (re)} over the central axis must be calculated, and equaled to the volume of the rectangular torus produced by the revolution of (S_p)^{axial (ri)} and (S_p)^{axial (ri)'}, in order to calculate the latter. Both volumes must be displaced a distance (r_i) of the center of the bar.

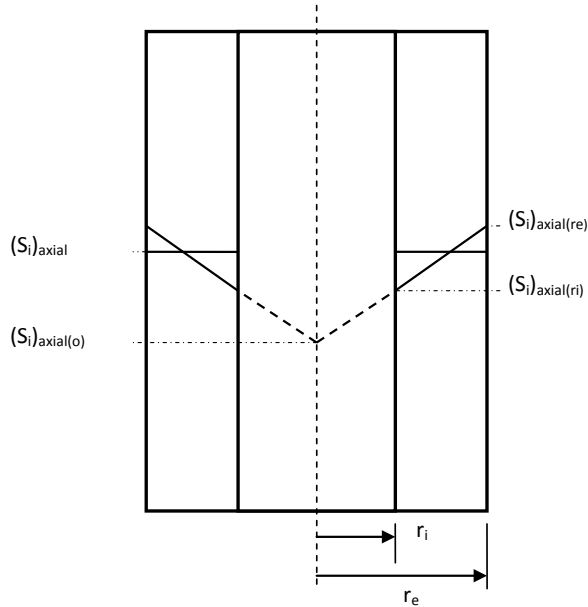


Figure 4. Stress distribution in a twisted hollow cylinder

Finally, the following relation can be written:

$$(\bar{S}_i)_{axial} = \frac{(S_i)_{axial(r)} \cdot \left(\frac{1}{3}r_e + \frac{2}{3}r_i\right) + (S_i)_{axial(e)} \cdot \left(\frac{1}{3}r_i + \frac{2}{3}r_e\right)}{(r_e + r_i)} \quad (19)$$

If (ri) tends to zero ((S_i)_{axial(r)} = (S_i)_{axial(0)}), the equation for the mean axial strength of a twisted solid cylindrical bar is obtained:

$$(\bar{S}_i)_{axial} = \frac{1}{3}(S_i)_{axial(0)} + \frac{2}{3}(S_i)_{axial(e)} \quad (20)$$

where (S_i)_{axial(0)} is the axial strength of the bar before torsion.

A graphic representation of the proposed methodology for the calculation of the axial yield strength can be observed in Figure 5.

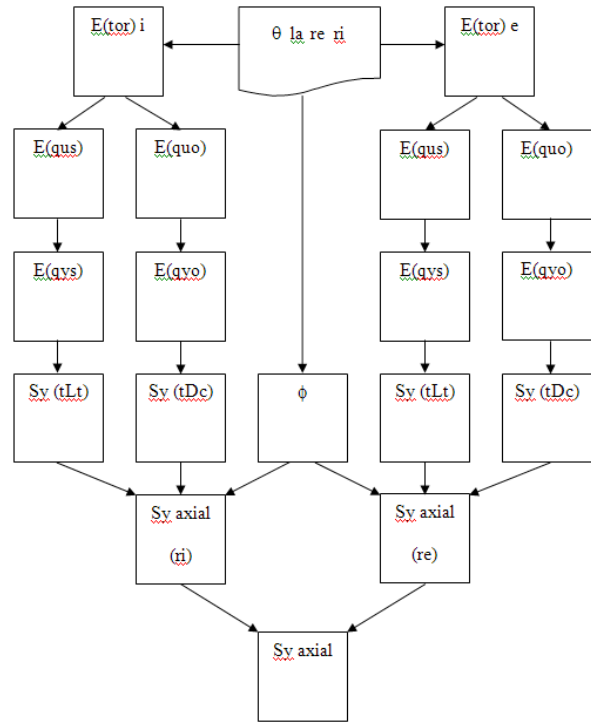


Figure 5. Schematic representation of the proposed methodology

Workpiece Material

Cylinders of approximately 170 mm in length with a diameter of 38.1 mm were cut from round bars of AISI 1020 steel (0.18 ± 0.01% C, 0.035 ± 0.001% S, and 0.40 ± 0.01% Mn) and AISI 1045 steel (0.455 ± 0.01% C and 0.82 ± 0.01% Mn). These steels were supplied in a cold-drawn state, and lengths of 3,000 mm.

Preparation of Work Specimens

The test specimens (Fig. 6) were machined to the required dimensions (Table 1) by turning in a CNC lathe, using ISO code - DCMT11T308MU carbide inserts with a nose radius of 0.8 mm. All the cutting processes were carried out with constant cutting parameters, and abundant quantity of water-soluble oil coolant, to ensure good surface quality [13, 14].

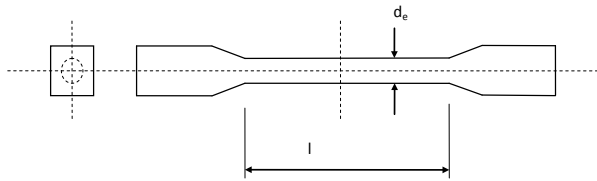


Figure 6. Torsion specimen's geometry and test dimensions

Table 1. Average test dimensions of the torsion specimens

Test	Solid (AISI 1045)		Hollow (AISI 1020)		
	d_e , mm	l , mm	d_i , mm	d_e , mm	l , mm
1	9.8	50	-	-	-
2	9.6	50	6.80	9.22	46.25
4	9.7	50	5.90	8.90	51.33
5	9.4	50	6.16	10.54	56.40
3	9.7	50	-	-	-

Heat Treatment

The samples were annealed at 870 °C for 1 h to get a fully recrystallized and untextured ferritic and pearlitic strain free structure. The mechanical properties, and work hardening equation obtained from tensile tests, done in accordance with the ASTM E8/E8M-13a standard [15], are shown in Table 2.

Table 2.

Mechanical properties and work hardening equation of the annealed AISI 1020 and AISI 1045 steel

Steel	S_y , MPa	S_u , MPa	$\sigma = \sigma_o(\epsilon)^m$, MPa
AISI 1020	268.90	434.34	$\sigma = 1012(\epsilon)^{0.26}$
AISI 1045	362.05	676.86	$\sigma = 1605(\epsilon)^{0.31}$

Torsion Tests

A free-end torsion machine was used for the torsion tests, in which the sample is deformed at a constant strain rate on the surface. AISI 1045 steel was twisted by applying angles of 90, 180, 270, 360 and 450 degrees, and 630, 720, 810 degrees for AISI 1020 steel, with five repetitions each.

From the twisted specimens, samples of AISI 1020 steel were drilled to remove the core and achieve the inner diameters (d_i) shown in Table 1. The process was carried

out using a lathe machine to ensure alignment with the axis of the specimen, with sufficient coolant and the appropriate cutting conditions to avoid changes in the surface integrity [16] of the material.

Tensile Tests

Tensile tests of the solid and hollow specimens, in accordance with the ASTM E8/E8M-13a standard [15], were performed to appreciate the material's strength limit variations resulting from the torsion process. Finally, the average yield and ultimate strength were calculated by discarding the values that were considerably outside the range demarcated by the other measures, and compared with those predicted by the proposed methodology.

Results and Discussion

For the evaluated conditions, the tensile tests and proposed methodology gave the following results.

As was expected the experimental and predicted axial yield and ultimate strength of solid cylindrical bars deformed by torsion increases with the angle of twist of the process, as shown in Table 3. This is because the superficial hardening of the material generated by the amount of induced plastic deformation, i.e. the development and distribution of strain and stress in the workpiece during the processing. Thus, the equivalent strain induced in the sample is proportional to the angle of twist.

The general tendency of the predicted axial yield and ultimate strength is to have higher values in hollow

cylinders, as shown in Table 4. This was also expected due to the removal of inner fibers with less plastic deformation. The strain hardening of the outer fibers is higher than that of the central ones, due to the proportionality of the plastic deformation with the radius. The hardening varies symmetrically about the center of processed specimens due to the lower imposed strain in the central area leading to lower hardening whereas higher plastic deformation is achieved at the peripheral area receiving a high imposed strain.

Table 3.

Experimental and predicted axial yield and ultimate strength of solid cylindrical AISI 1045 bars deformed by torsion

Angle of twist, degrees	S_y , MPa			S_u , MPa		
	Experimental	Predicted	Error, %	Experimental	Predicted	Error, %
90	542.31	549.01	1.22	706.08	703.41	0.38
180	617.82	638.62	3.26	726.97	729.35	0.33
270	657.05	698.45	5.93	761.98	757.19	0.63
360	671.76	735.85	8.71	763.45	781.48	2.31
450	696.27	771.73	9.78	826.01	863.42	4.33

It can be seen in Tables 3 and 4 that the proposed model adjusted very well to the experimental values, with maximum errors of 9.78% for solid cylinders, and 6.81% for hollow cylinders, which highlights the good accuracy of the method.

Table 4.

Experimental and predicted axial yield and ultimate strength of solid and hollow cylindrical AISI 1020 bars deformed by torsion

Angle of twist, degrees	S_y , MPa				S_u , MPa			
	Solid	Hollow			Solid	Hollow		
	Predicted	Experimental	Predicted	Error, %	Predicted	Experimental	Predicted	Error, %
630	560.29	643.23	690.23	6.81	652.97	677.55	699.08	3.08
720	559.89	640.38	684.01	6.38	652.32	655.07	694.21	5.64
810	572.22	671.74	698.13	3.78	673.19	698.14	715.82	2.47

Conclusions

In relation to the proposed methodology and experimental conditions evaluated in this work the following conclusions can be drawn from the results:

(1) A relatively simple methodology for the prediction of axial yield and ultimate strength based on the assumption of an angle of twist of annealed solid and hollow cylindrical bars was presented.

(2) When the angle of twist of the torsion process increases, the axial yield and ultimate strength also increase.

(3) After the torsion process, hollow cylindrical bars have higher predicted values of the axial yield and ultimate strength as compared with solid cylinders.

(4) The proposed formulation gives acceptable results, with errors not greater than 9.78 and 6.81% for solid and hollow cylinders, respectively.

References

- [1] Knap, F. "Twisting Wire and Round Bar to Increase Strength", *Wire World Int.*, Vol. 29, No. 4, (1987), 94-96.
- [2] Yang, Z. and Welzel, U. "Microstructure-microhardness Relation of Nanostructured Ni Produced by High-pressure Torsion", *Mater. Lett.*, Vol. 59, No. 27, (2005), 3406-3409.
- [3] Horita, Z. and Langdon, T. "Microstructures and Microhardness of an Aluminum Alloy and Pure Copper After Processing by High-pressure Torsion", *Mat. Sci. Eng. A*, Vol. 410-411, (2005), 422-425.
- [4] Janecek, M. Krajnák, T. Stráská, J. Cízek, J. Lee, D.J. Kim, H.S. and Gubicza, J. "Microstructure Evolution in Ultrafine-grained Interstitial Free Steel Processed by High Pressure Torsion", *IOP Conf. Ser.: Mater. Sci. Eng.*, Vol. 63, (2014), 12055-12063.

- [5] Huang, Y. Maury, N. Zhang, N.X. and Langdon, T.G. "Microstructures and Mechanical Properties of Pure Tantalum Processed by High - Pressure Torsion", IOP Conf. Ser.: Mater. Sci. Eng., Vol. 63, (2014), 12100-12107.
- [6] Jiang, B.Z. Emura, S. and Tsuchiya, K. "Microstructures and Mechanical Properties of Ti5553 Alloy Processed by High-pressure Torsion", IOP Conf. Ser.: Mater. Sci. Eng., Vol. 63, (2014), 12069-12075.
- [7] Canova, G. Shrivastava, S. Jonas, J. and G'sell, C. "The Use of Torsion Testing to Assess Material Formability", ASTM Spec. Tech. Publ., Vol. 753, (1982), 189-210.
- [8] Batdorf, S. and Ko Robert, W. "Shear Plastic Stress-strain Relation Obtained from Torque-twist Data", J. Eng. Mater-T, Vol. 108, No. 4, (1986), 354-357.
- [9] Hematiyan, M.R. and Doostfatemeh, A. "Torsion of Moderately Thick Hollow Tubes with Polygonal Shapes", Mech. Res. Commun., Vol. 34, No. 7/8, (2007), 528-537.
- [10] Yang, Z. Li, X. and Yang, J. "Interpretation of Torsional Shear Results for Nonlinear Stress-strain Relationship", Int. J. Numer. Anal. Met., Vol. 32, No. 10, (2007), 1247-1266.
- [11] Datsko, J. Materials Selection for Design and Manufacturing: Theory and Practice, Marcel Dekker, Inc., New York, 1997.
- [12] Weisstein, E. Concise Encyclopedia of Mathematics, 2nd ed., CRC Press, New York, 2003
- [13] Hussein, S.G. "An Experimental Study of the Effects of Coolant Fluid on Surface Roughness in Turning Operation for Brass Alloy", J. Eng., Vol. 20, No. 3, (2014), 96-104.
- [14] Deepak, D. and Rajendra, B. "Investigations on the Surface Roughness Produced in Turning of Al6061 (As-Cast) by Taguchi Method", Int. J. Res. Eng. Technol., Vol. 04, No. 08, (2015), 295-298.
- [15] ASTM E8/E8M-13a, Standard Test Methods for Tension Testing of Metallic Materials, ASTM International, West Conshohocken, PA, 2013.
- [16] Field, M. and Kahles, J. "Review of Surface Integrity of Machined Components", Ann. CIRP, Vol. 20, (1971), 153-163.

Recibido el 09 de Junio de 2017

En forma revisada el 01 de Marzo de 2018



UNIVERSIDAD
DEL ZULIA

REVISTA TECNICA

DE LA FACULTAD DE INGENIERIA
UNIVERSIDAD DEL ZULIA

Vol. 41. N°2, Mayo - Agosto 2018_____

*Esta revista fue editada en formato digital y publicada en Abril de 2018, por el **Fondo Editorial Serbiluz**, Universidad del Zulia. Maracaibo-Venezuela*

www.luz.edu.ve
www.serbi.luz.edu.ve
produccioncientifica.luz.edu.ve